Protection against severe infant lower respiratory tract infections by immune training: Mechanistic studies

Niamh M. Troy, BSc,[a] Deborah Strickland, PhD,[a] Michael Serralha, BSc,[a] Emma de Jong, PhD,[a] Anya C. Jones, PhD,[a] James Read, BSc,[a] Sally Galbraith, MSc,[c] Zahir Islam, PhD,[c] Parwinder Kaur, PhD,[b] Kyle T. Mincham, PhD,[d] Barbara J. Holt, BSc,[a] Peter D. Sly, PD, DSc,[c] Anthony Bosco, PhD,[e] and Patrick G. Holt, DSc[a] *Perth and Brisbane, Australia; London, United Kingdom; and Tucson, Ariz*

GRAPHICAL ABSTRACT

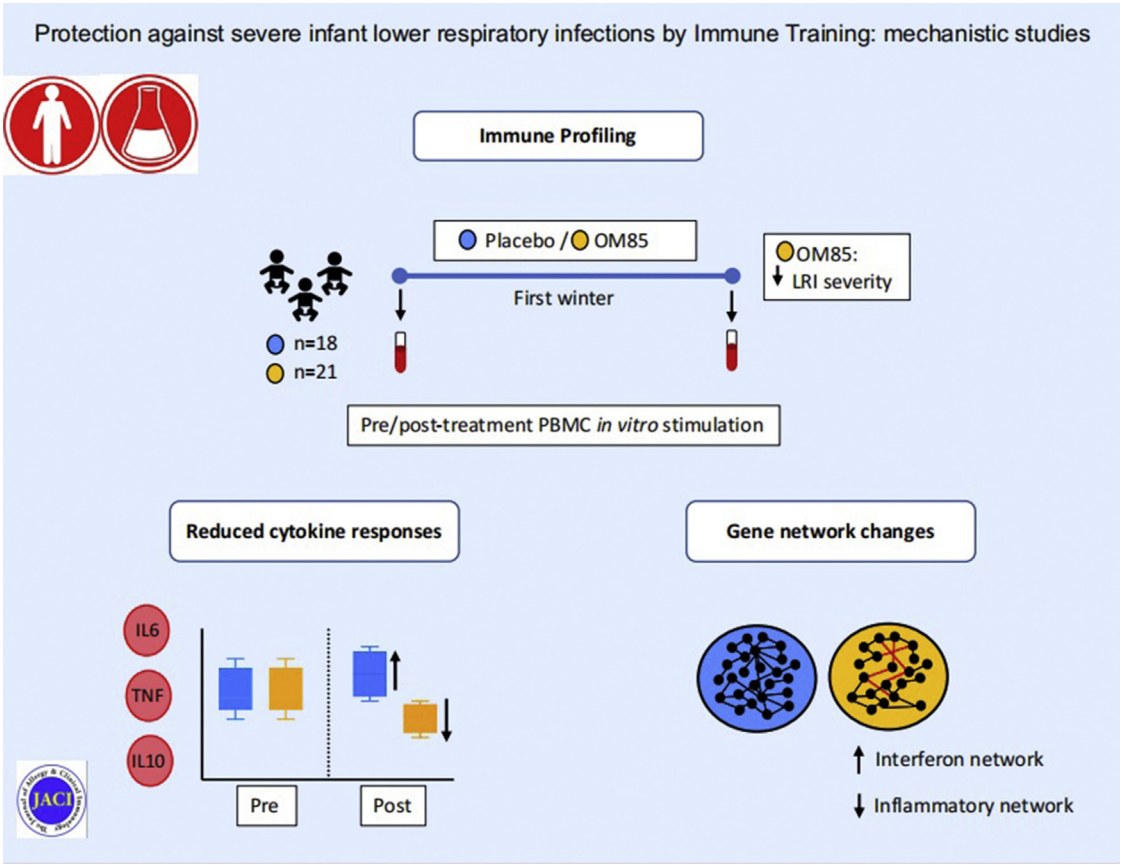

Background: Results from recent clinical studies suggest potential efficacy of immune training (IT)-based approaches for protection against severe lower respiratory tract infections in infants, but underlying mechanisms are unclear.

Objective: We used systems-level analyses to elucidate IT mechanisms in infants in a clinical trial setting.
Methods: Pre- and posttreatment peripheral blood mononuclear cells from a placebo-controlled trial in which winter treatment with the IT agent OM85 reduced infant

From [a]the Telethon Kids Institute and [b]the School of Agriculture and Environment, The University of Western Australia, Perth; [c]the Child Health Research Centre, University of Queensland, Brisbane; [d]the National Hearth and Lung Institute, Imperial College London, London; and [e]Asthma and Airway Disease Research Center, The University of Arizona, Tucson.

The last 2 authors contributed equally to this article, and both should be considered senior author.

This study was funded by the National Health and Medical Research Council of Australia. N.M.T. is supported by a Mickie Hardy scholarship from Asthma Australia. OM Pharma, Switzerland, provided OM85 and placebo but had no input into trial design, study conduct, or data analysis.

Disclosure of potential conflict of interest: The authors declare that they have no relevant conflicts of interest.

Received for publication May 4, 2021; revised December 23, 2021; accepted for publication January 10, 2022.

Corresponding author: Patrick G. Holt, DSc, Telethon Kids Institute, Northern Entrance, Perth Children's Hospital, 15 Hospital Ave, Nedlands WA 6009, Perth, Australia. E-mail: patrick.holt@telethonkids.org.au.

0091-6749/$36.00

https://doi.org/10.1016/j.jaci.2022.01.001

respiratory infection frequency and/or duration were stimulated for 24 hours with the virus/bacteria mimics polyinosinic:polycytidylic acid/lipopolysaccharide. Transcriptomic profiling via RNA sequencing, pathway and upstream regulator analyses, and systems-level gene coexpression network analyses were used sequentially to elucidate and compare responses in treatment and placebo groups.

Results: In contrast to subtle changes in antivirus-associated polyinosinic:polycytidylic acid response profiles, the bacterial lipopolysaccharide-triggered gene coexpression network responses exhibited OM85 treatment–associated upregulation of IFN signaling. This was accompanied by network rewiring resulting in increased coordination of *TLR4* expression with IFN pathway–associated genes (especially master regulator *IRF7*); segregation of TNF and *IFN-γ* (which potentially synergize to exaggerate inflammatory sequelae) into separate expression modules; and reduced size/complexity of the main proinflammatory network module (containing, eg, *IL-1, IL-6,* and *CCL3*). Finally, we observed a reduced capacity for lipopolysaccharide-induced inflammatory cytokine (eg, IL-6 and TNF) production in the OM85 group.

Conclusion: These changes are consistent with treatment-induced enhancement of bacterial pathogen detection/clearance capabilities concomitant with enhanced capacity to regulate ensuing inflammatory response intensity and duration. We posit that IT agents exemplified by OM85 potentially protect against severe lower respiratory tract infections in infants principally by effects on innate immune responses targeting the bacterial components of the mixed respiratory viral/bacterial infections that are characteristic of this age group. (J Allergy Clin Immunol 2022;■■■:■■■-■■■.)

Key words: *Severe lower respiratory tract infections, immune training, transcriptomics, infants, peripheral blood mononuclear cells, gene coexpression networks*

Abbreviations used
DEG: Differentially expressed genes
DGCA: Differential gene correlation analysis
IT: Immune training
LPS: Lipopolysaccharide
PBMC: Peripheral blood mononuclear cells
PIC: Polyinosinic:polycytidylic acid
sLRI: Severe lower respiratory tract infections
TLR: Toll-like receptor
URA: Upstream regulator analysis

Development of effective therapeutic strategies for protection against severe lower respiratory tract infections (sLRI) during the high-risk infant period remains a crucial unmet need in pediatrics. A number of interacting factors complicate this challenge, in particular the broad spectrum of pathogens involved;[1-3] the restricted coverage of these provided by currently available vaccines;[4] and developmental constraints that limit the capacity of the infant immune system to respond efficiently to conventional vaccines that target T- or B-cell memory.[4] Adding further complexity, while developmentally compromised IFN-dependent innate immunity during this period is also recognized as an important risk factor predisposing to sLRI,[5] the most severe manifestations of this disease in infants are associated with hyperexpression of IFN responses in the airways.[6,7]

This window of susceptibility in early life has implications beyond direct infection-associated morbidity and mortality, given the growing understanding that episodic infant sLRI can also enhance risk for later development of complex diseases, including chronic asthma[8] and chronic obstructive pulmonary disease.[9] The emerging concept of immune training (IT) provides an potential avenue for addressing this challenge. IT involves stimulation of long-lasting augmented innate immune function after controlled exposure to microbe-derived stimuli, manifesting in enhanced resistance to pathogens unrelated to the original stimulus.[10,11] Maintenance of this broad-spectrum "innate immune memory" state appears to involve both epigenetic mechanisms and changes in the phenotypes/population size of key myeloid precursors.[11] The neonatal and infant periods appear to represent life phases during which the immune system is particularly susceptible to microbe-associated IT effects.[10-12]

Opportunities for clinical studies evaluating this concept and elucidating underlying mechanisms are currently limited as a result of the restricted range of IT treatment agents with proven safety in this age group. The present study focuses on one such available agent, OM85, which comprises a polybacterial extract from a mixture of respiratory pathogens that have been in clinical use since the 1980s. A number of clinical studies on OM85 have reported protection against early-life lower respiratory tract infections,[13,14] and these have provided the impetus for more recent randomized controlled trials supported by funding agencies, including the US National Institutes of Health[15] and the Australian National Health and Medical Research Council.[16] Data from experimental animal models data suggest that OM85 treatment may operate via effects on immunoregulatory myeloid/lymphoid cell populations that calibrate innate immune responses to microbial stimuli.[17-20] However, corresponding IT mechanisms in human infants remain to be elucidated, and this represented the aim of the present study on the immunomodulatory effects of OM85 treatment across the first winter.

We used an experimental design and analytic strategy to assess viral/bacterial responses on the basis of previous findings on patterns of episodic upper or lower respiratory tract infections in birth cohorts followed throughout infancy to age 5 years.[1-3] These studies demonstrated that nasopharyngeal bacteriomes/viromes collected during symptom episodes typically contained not only a viral pathogen or pathogens, but also 1 or more common bacterial pathogens.[1-3] Moreover, the presence of bacterial pathogens enhanced risk for infection spread to the lower airways, with accompanying symptom intensification.[1] We reasoned that underlying host innate immunoinflammatory responses during early sLRIs would thus be directed against both pathogen classes. We accordingly developed a 2-tiered analytic approach to elucidate transcriptomic profiles in peripheral blood mononuclear cells (PBMC) from OM85-treated and placebo groups triggered by the virus mimic polyinosinic:polycytidylic acid (PIC), also known as Poly(I:C), and the bacteria mimic lipopolysaccharide (LPS) to test the hypothesis that treatment would alter the structure of underlying group-specific gene coexpression networks.

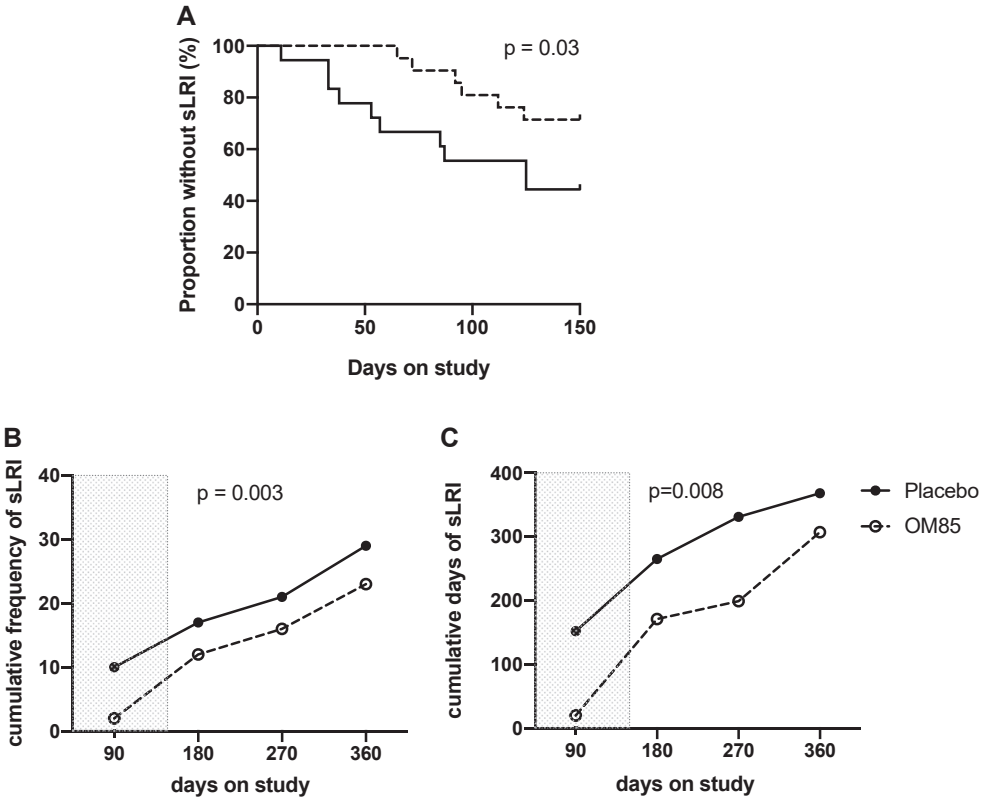

FIG 1. sLRIs in subjects with available PBMC. **A**, Time to first sLRI during treatment period; Kaplan-Meier survival analysis performed by Gehan-Breslow test. **B** and **C**, Cumulative frequency of sLRI per number of days with sLRI during the first year; 2-way ANOVA. Shaded areas in (*B*) and (*C*) indicate treatment period. *Dashed line,* OM85 group (n = 21); *solid line,* placebo group (n = 18).

METHODS

Subjects

Subjects comprised infants at high risk for asthma development who participated in a placebo-controlled clinical trial that demonstrated significant reduction in susceptibility to sLRI resulting from daily OM85 (3.5 mg; OM Pharma, Geneva, Switzerland) treatment throughout their first winter.[16] The present investigation was restricted to a subset of this cohort from whom PBMC was collected in year 1 for mechanistic studies (see Fig E1 in this article's Online Repository available at www.jacionline.org) and who were representative of the overall cohort (see Table E1 in this article's Online Repository). Ethical approval was provided by Children's Health Queensland and the University of Queensland (reference HREC/12/QRCH/119), and at least 1 parent or guardian provided written consent.

PBMC processing

Peripheral blood was collected before and after OM85 treatment or placebo. PBMC were isolated and cryobanked as previously described.[21]

In vitro investigations

PBMC were cultured in RPMI (Gibco, Waltham, Mass) 1640 with 10% fetal calf serum alone (control) or with the addition of PIC (50 μg/mL, InvivoGen, San Diego, Calif) or LPS (25 pg/mL; Enzo Life Sciences, Farmingdale, NY) for 24 hours. Supernatants were collected after culture and stored at −80°C for cytokine quantification by Luminex (R&D Systems, Minneapolis, Minn).

Flow cytometry

Immunostaining of 1×10^6 viable PBMC was performed using a panel of monoclonal antibodies,[22] as detailed in the Online Repository available at www.jacionline.org.

Transcriptomics

Total RNA was extracted from PBMC after culture using TRIzol (Invitrogen, Waltham, Mass) and purified using the RNEasy MinElute Kit (Qiagen, Hilden, Germany). Sequencing libraries were prepared using TruSeq Stranded mRNA Sample Prep Kit (Illumina, San Diego, Calif) following the manufacturer's instructions. Data before processing and quality control are provided in the Online Repository available at www.jacionline.org. RNA sequencing data are available from the National Center for Biotechnology Information (NCBI) Gene Expression Omnibus repository (accession no. GSE184487).

Differential expression analysis

Differentially expressed genes (DEG) were identified by EdgeR,[23] which uses a negative binomial distribution model, with Benjamini-Hochberg–adjusted false discovery rate. Unwanted variation was modeled and adjusted for by RUVSeq, as shown in the Online Repository available at www.jacionline.org. DEGs were identified in response to PIC or LPS versus paired unstimulated controls at time points before and after treatment. Genes with an absolute log fold change of >1.5 and a false discovery rate of <0.05 were considered to be differentially expressed.

Network analysis

Network analysis was performed using WGCNA,[24] and network reconstruction was performed by Ingenuity Systems,[25] as described in previous publications.[17,21,25,26] Methods are provided in the Online Repository available at www.jacionline.org.

Pathway analysis

Pathway analysis was performed on differentially DEG using InnateDB,[27] which utilizes the public databases INOH, KEGG, NETPATH, PID,

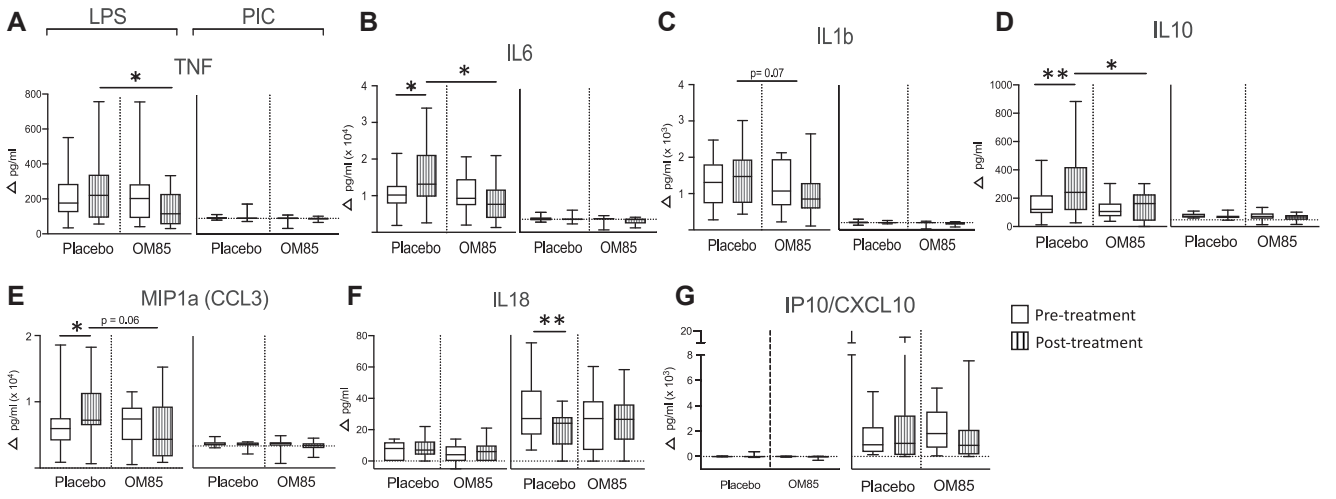

FIG 2. PBMC cytokine responses to LPS (*left*) and PIC (*right*) measured by Luminex multiplex assay in 24-hour culture supernatants from placebo (n = 16 pairs) and OM85 (n = 18 pairs). *White boxes,* before treatment; *vertical stripes,* after treatment. Within-group comparisons, Wilcoxon test; between-group comparisons, Mann-Whitney test. $*P < .05$, $**P < .005$. The Δ_{data} was baseline corrected (PIC/LPS − Control) for each subject.

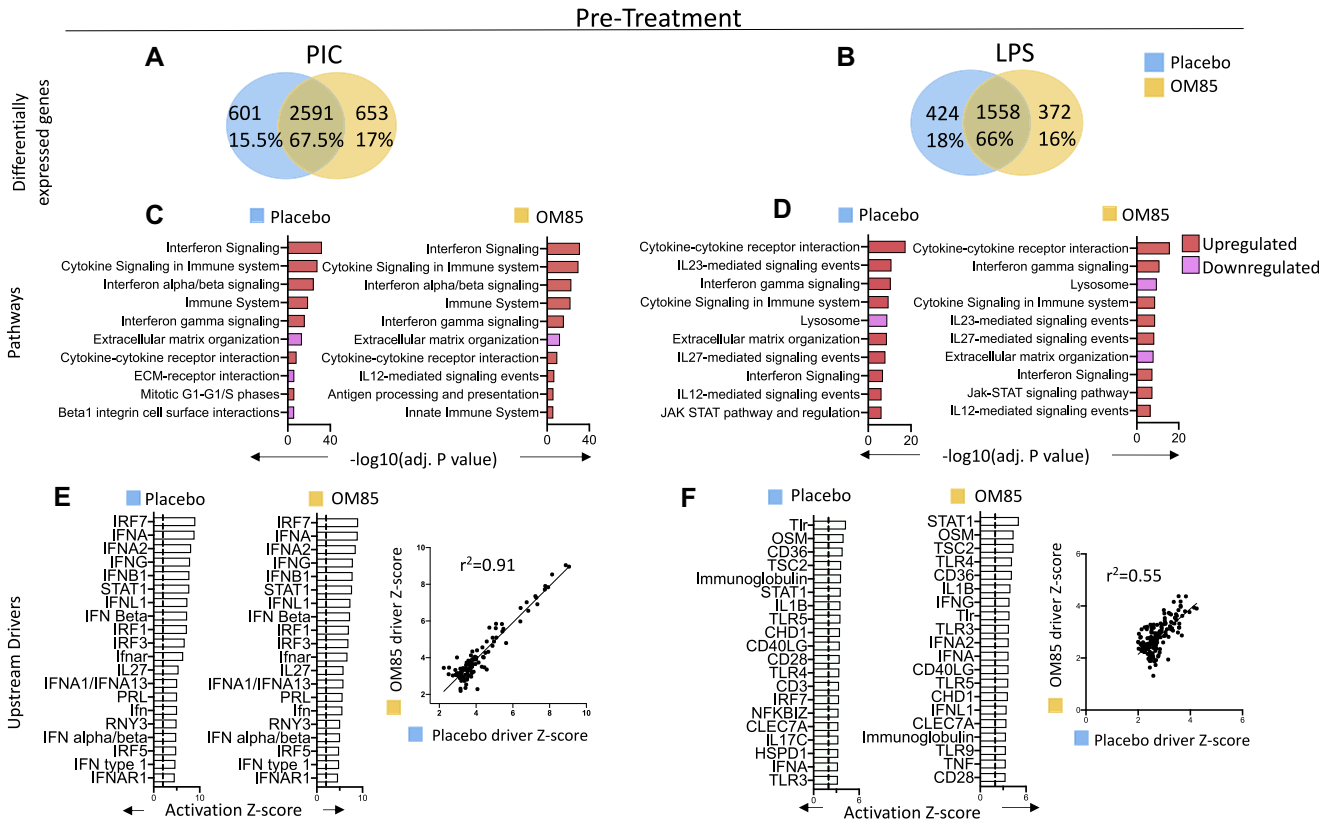

FIG 3. Group responses to PIC and LPS at time of recruitment. DEG were identified in response to PIC/LPS in placebo (*blue,* n = 16/15) and OM85 (*yellow,* n = 16/15). **A** and **B**, Venn diagrams showing the overlap of DEGs between groups. **C** and **D**, Top 10 significant pathways enriched in upregulated (*red*) and downregulated (*pink*) DEGs using InnateDB. Benjamini-Hochberg–adjusted $P < .05$ was considered statistically significant. **E** and **F**, Predicted upstream regulators of PIC/LPS responses and their correlations between groups. Absolute activation *z* scores >2.0 and Benjamini-Hochberg–adjusted $P < .05$ were deemed significant.

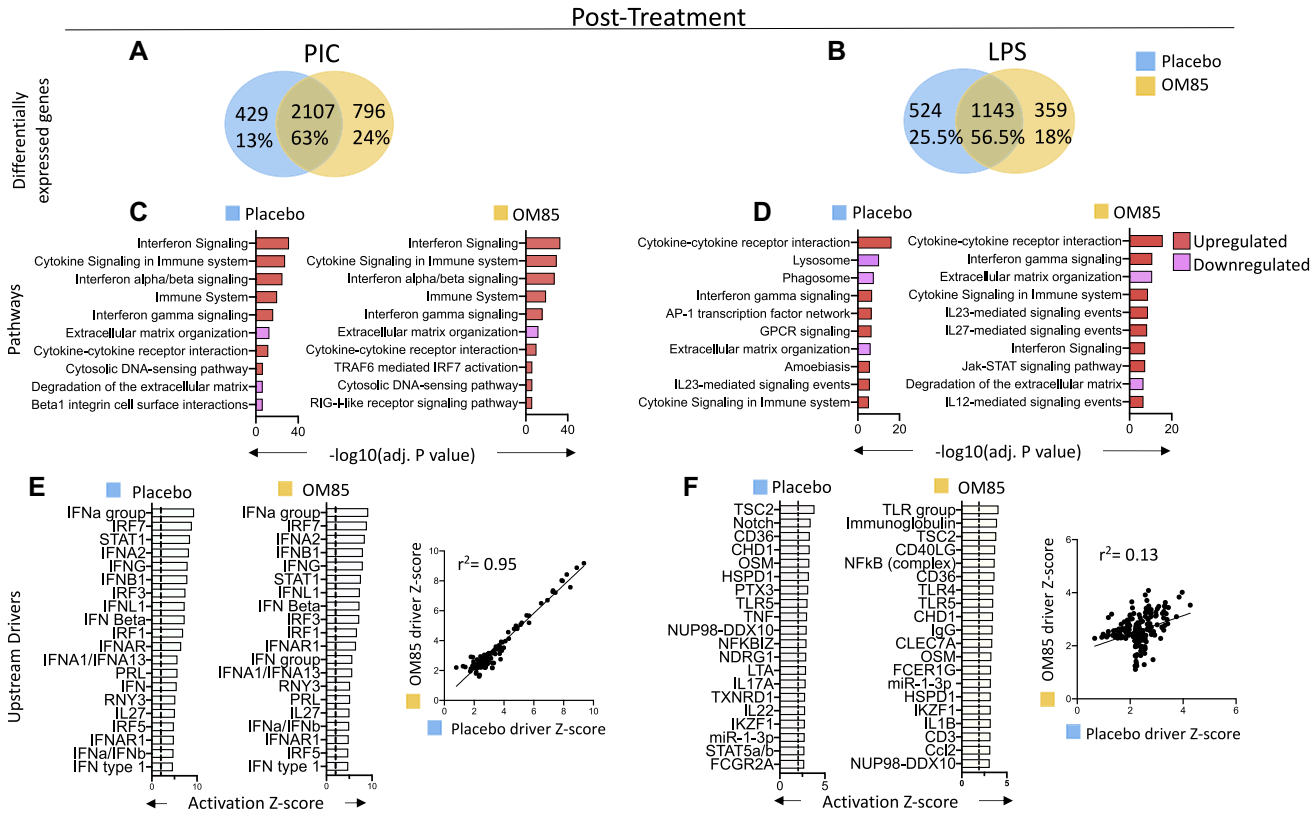

FIG 4. Group responses to PIC/LPS after treatment in placebo (*blue*, n = 15/16) and OM85 (*yellow*, n = 17/16). **A** and **B**, Venn diagrams showing the overlap of DEGs between groups. **C** and **D**, Top 10 significant pathways enriched in upregulated (*red*) and downregulated (*pink*) DEGs using InnateDB. **F** and **G**, Predicted upstream regulators of PIC/LPS responses and their correlations between groups. Statistics applied are consistent with Fig 3.

BIOCARTA, and REACTOME. Up- and downregulated genes were analyzed separately; we discuss the 10 most significant pathways. The ReactomePA package in R[28] was utilized to identify/visualize pathways enriched in network modules, and were confirmed using InnateDB.

Upstream regulator analysis

For upstream regulator analysis (URA), Ingenuity Systems[29] was used to identify putative drivers of gene expression changes and network module activity (see the Online Repository available at www.jacionline.org).

Differential gene correlation analysis

The differential gene correlation analysis (DGCA) R package[30] was used to discover gene pairs in the network that were differentially correlated in OM85 treatment compared to placebo in LPS and PIC responses separately. Permutation testing was performed to determine significance between groups; adjusted $P < .05$ was considered statistically significant.

RESULTS

Clinical responses of study subjects to OM85 treatment

As noted in the Methods, study subjects comprised a subgroup from a clinical trial comparing sLRI susceptibility of OM85- versus placebo-treated infants across their first winter (Fig E1), the results of which have been published elsewhere.[16] OM85-treated subjects in this subgroup demonstrated a longer time to first sLRI during the treatment period compared to their placebo counterparts ($P = .03$, Fig 1, *A*). This was accompanied by reduced cumulative frequency of sLRI events ($P = .003$, Fig 1, *B*) and fewer days of sLRI symptoms ($P = .008$, Fig 1, *C*), closely mirroring the clinical findings from the whole cohort.[16]

Cytokine responses

The OM85 group produced significantly lower levels of proinflammatory cytokines (TNF $P = .03$; IL-6 $P = .01$; IL-10 $P = .03$), and trended lower for IL-1β ($P = .07$) and CCL3/MIP1α ($P = .06$) in the LPS response. Furthermore, OM85 treatment constrained the age-related increase in LPS-associated inflammatory cytokine response capacity that was evident in the placebo group (Fig 2, *B-E*). IL-18 and IP10 were produced in response to PIC but were unaffected by OM85 treatment (Fig 2, *F* and *G*).

Transcriptional responses to PIC and LPS in placebo and OM85 treatment groups before versus after treatment

PIC and LPS induced strong perturbations to the gene expression program (see Fig E2, *A*, in the Online Repository available at www.jacionline.org), as reflected in DEG signatures in both groups at the start of the study (before treatment), with comparably strong overlap between respective response profiles

(Fig 3, *A* and *B*). The observed transcriptional responses were clustered by stimulus (Fig E2, *B* and *C*) and include known antiviral genes (eg, *MX1, IFNa1, CXCL10*) upregulated in response to PIC and inflammatory genes (*IL-6, IL-1β, CSF3*) in response to LPS (see Tables E2-E5 in the Online Repository). Pathway analysis revealed that the most prominent DEG signatures in PIC and LPS responses in both groups were associated with IFN and cytokine signaling (Fig 3, *C* and *D*), reflecting the overlap in Fig 3, *A* and *B*. Using URA to infer master regulators operating upstream of the transcriptional changes suggested that the top 20 drivers of PIC responses were identical in the 2 groups and differed only subtly in *z* scores. The identified drivers of the PIC response were dominated by genes associated with type 1/2/3 IFN responses (Fig 3, *E*), with a slightly more diverse array in the LPS responses that included proinflammatory cytokines (*OSM, IL-1β*) and those associated with Toll-like receptor (TLR) functions including the regulator TSC2[31] (Fig 3, *F*). Furthermore, the top 150 drivers of both responses correlated strongly between groups (PIC stimulation $r^2 = 0.91$; LPS stimulation $r^2 = 0.55$; Fig 3, *E* and *F*).

Posttreatment transcriptomic responses to PIC/LPS were not superficially different between OM85 and placebo groups (Fig 4, *A* and *B;* and see Fig E2, *A,* and Tables E6-E9 in the Online Repository at www.jacionline.org), and principal component analysis/hierarchical clustering confirmed that samples cluster primarily by stimulus and not by treatment group (Fig E2, *B* and *D*). Pathway analysis indicated that gene signatures associated with IFN/cytokine signaling remained dominant in the response profiles (Fig 4, *C* and *D*). However, the LPS profile included a secondary tier of signatures (including *AP-1* transcription factor pathway, *GPCR*, *Jak-STAT*, and *IL-27* signaling), which were distributed differently between groups (Fig 4, *D*).

Consistent with the prominence of cytokine/IFN signaling in PIC responses (Fig 4, *D*), URA demonstrated that upstream driver profiles were dominated by type 1/2/3 IFN-associated genes (Fig 4, *E*), which overall correlated strongly between groups ($r^2 = 0.95$). The intragroup variations in LPS-responsive pathways (Fig 4, *D*) were mirrored by some notable differences in respective ranked lists of upstream drivers, in particular the increased prominence of TLR signaling in the treatment group and the presence of TNF (the principal AP-1 driver) among the main drivers in the placebo group (Fig 4, *F*). These variations were reflected by much weaker correlation between respective driver profiles ($r^2 = 0.13$).

Coexpression network analysis

Transcriptional responses to PIC and LPS included multiple shared DEGs equating to >50% overlap (see Fig E3 in the Online Repository available at www.jacionline.org), consistent with previous reports.[32] Therefore, to characterize OM85 treatment effects at the systems level, we combined respective group-specific PIC, LPS, and control data to construct separate posttreatment gene networks for each group using WGCNA. First, to determine if there were broad treatment-associated changes in global gene network topology, we calculated ranked gene expression and gene connectivity (coexpression) across network genes before and after treatment. PIC network connectivity patterns correlated strongly between groups at each time point (before/after $r^2 = 0.63/0.66$; see Fig E4 in the Online Repository), indicating conservation of antivirus-specific network patterns over time with or without OM85 treatment. In contrast, in the LPS response, gene connectivity was more variable after treatment ($r^2 = 0.4$) relative to before treatment ($r^2 = 0.62$; Fig E4), suggesting that treatment-induced changes to the network structure focused primarily on the antibacterial arm of the innate response. Next, we looked at the global topology and connectivity structure of the coexpression networks underlying innate immune responses using WGCNA. The placebo network was organized into 5 coexpression modules, versus 8 modules in the OM85 group, suggesting increased network architecture complexity with treatment (see Fig E5, *A,* and Tables E10 and E11 in the Online Repository). We used ReactomePA to annotate the modules, and the 5 most significant pathways in each are shown in Table E12 in the Online Repository.

As shown in Fig 4, the response profiles in both groups were driven primarily by IFN-related and cytokine/chemokine signaling, and the majority of genes that regulate these processes fit into 1 of 3 of coexpression modules A, B, and C (Table E12); we focus in detail on these in Fig 5. In both groups, module A was enriched with type 1/2/3 IFN, and module C was enriched with cytokine signaling pathways. Module B was unique to the OM85 group and showed some overlapping functions with module A (Fig 5, *A*). Of note, 147 of the 211 genes making up module B in the OM85 group were present in module A in the corresponding placebo network (Fig 5, *B*), and similar levels of treatment-associated gene translocation were observed between modules C and D.

To determine how the network modules were expressed within the 2 groups after LPS/PIC stimulation, we plotted module eigengene values (which summarize the overall activity of each coexpression module) for each response and compared them with paired unstimulated controls (Fig E5, *D*). Findings related to modules A through C (Fig 5, *C*) are discussed below, while those relating to modules D through H are shown in Fig E5, *B,* but are not considered further. Module A (*blue*) was upregulated in response to PIC relative to paired controls in both groups, but in the LPS response upregulation was restricted to the OM85 group (Fig 5, *C*). The upstream drivers of module A/PIC response displayed a high degree of overlap and comparable activation *z* scores in the 2 groups, and the driver profile was dominated by IFN-associated genes (Fig 5, *D*). In contrast, the top drivers of module A/LPS response differed markedly between placebo and treatment groups, most notably by the absence of classical innate immunity/IFN-related drivers of the LPS response in the placebo group (Fig 5, *D*). This finding is further highlighted in Fig E6 (available in the Online Repository available at www.jacionline.org), which compares activation *z* scores for a broad list of IFN/TLR-related and associated immunomodulatory genes that are significant drivers of module A/LPS responses in the treatment, but not placebo, group. Reconstruction of a representative wiring diagram (using Ingenuity Pathway Analysis[29]) of so-called interferon module A revealed that *IFN-γ, STAT1, IRF7*, and *IRF1* were hubs in both placebo and OM85 response networks. However, the placebo network module A also included *TNF* and *MYD88* hubs, which were absent from the corresponding OM85 module (see Fig E7, *A,* in the Online Repository). A subset of genes in module A in the placebo group were partitioned into a separate small (n = 211) module B (*pink*) in the OM85 group, and reconstruction of this module showed that *TNF* and *MYD88* had translocated from module A to B, in which they were present as hubs (Fig E7, *A*). In addition to uncoupling of

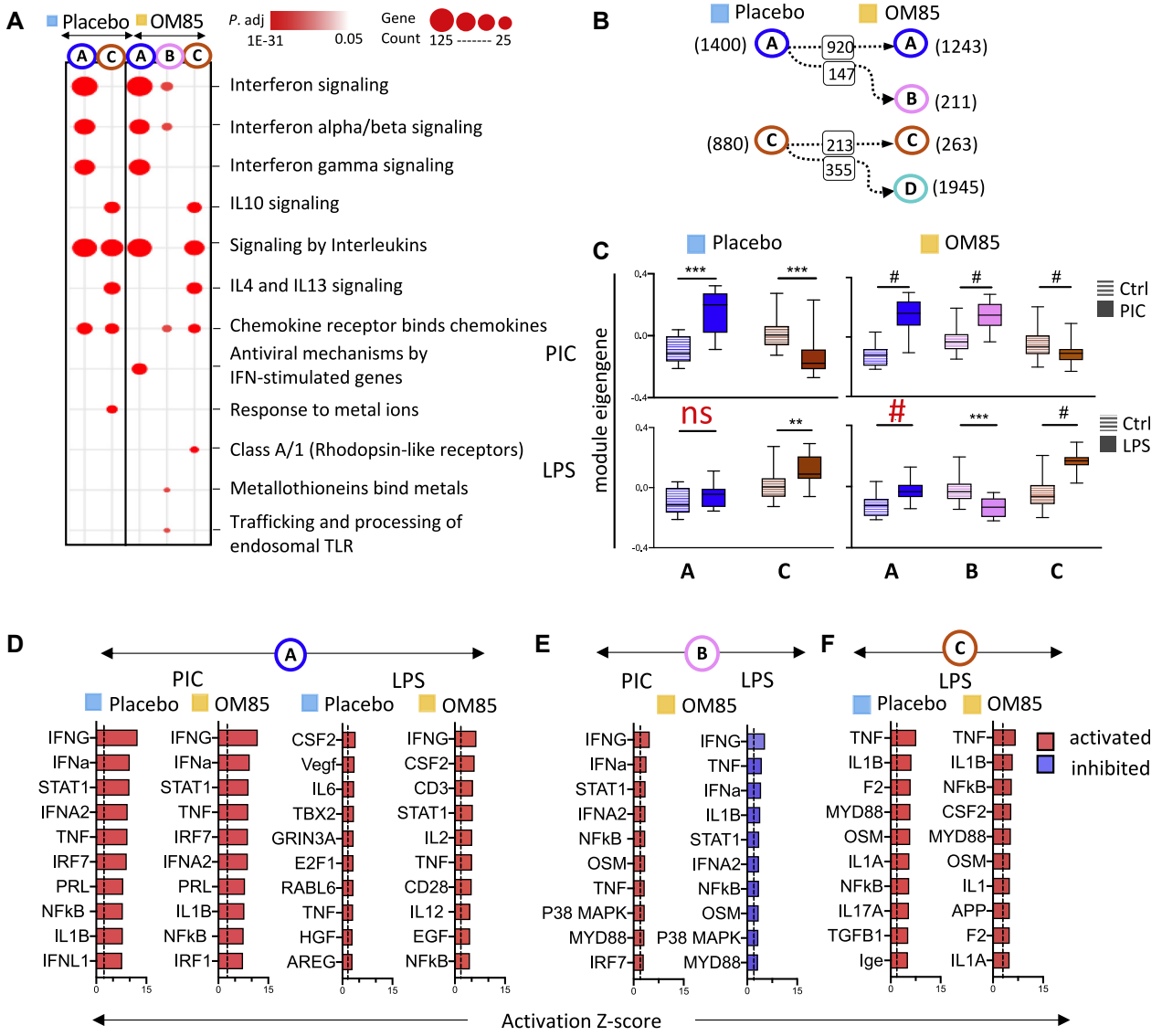

FIG 5. A-C, Gene modules of interest in placebo/OM85 gene networks underlying innate immune responses to PIC/LPS in PBMC. Gene coexpression networks that were constructed separately for placebo (*blue*) and OM85 (*yellow*) groups by combining PIC/LPS and control (CTR) data (placebo n = 47, OM85 n = 51). *A,* Top 5 significant (adjusted $P < .05$) pathways enriched in gene modules A, B, and C derived using ReactomePA. *B,* Road map demonstrating changes in gene distribution patterns with OM85 treatment. *C,* Network module responses were determined by plotting module eigengenes for PIC/LPS (*top/bottom, solid boxes*) and were compared to paired controls (*striped boxes*) for placebo (*left*) and OM85 (*right*). $^{**}P < .005$, $^{***}P < .0005$, #$P <$ .0001, Wilcoxon test. **D-F**, Top 10 predicted drivers of module A (placebo/OM85 to PIC [*left*] and LPS [*right*]), module B (only in OM85 network), and module C in LPS response. *Red* and *blue* indicate, respectively, activated and inhibited drivers. Absolute activation *z* score >2.0 and Benjamini-Hochberg–adjusted $P < .05$ were deemed significant.

TNF from interferon module A, LPS-induced production of TNF protein was reduced in the OM85 group after treatment ($P = .03$), as previously noted (Fig 2, *A*). In contrast, URA, which identifies upstream driver genes, suggested that production of TNF played an active role earlier in the responses of both groups (Fig 5, *D*).

In the OM85 network only, module B was upregulated in the PIC response versus equivalently downregulated in the LPS response (Fig 5, *C*). Upstream drivers for module B (Fig 5, *E*) overlap strongly with those for module A (Fig 5, *D*). Moreover, consistent with the reciprocal module activation patterns in Fig 5, *C,* the top drivers of this module display positive activation *z* scores in the PIC response versus negative scores for LPS (Fig 5, *E*). Finally, module C (*brown*) was upregulated in the LPS response in both groups (Fig 5, *C*) and was driven by proinflammatory cytokines including TNF, IL-1β, and IL-6 (Fig 5, *F*). Reconstruction of module C demonstrated major reduction in module size and/or complexity in the OM85 treatment group, which included translocation of a large block of genes (n = 355) from OM85 treatment modules C to D (Fig 5, *B*). Proinflammatory genes *IL-6, IL-1β*, and *CSF2* and immunoregulatory gene

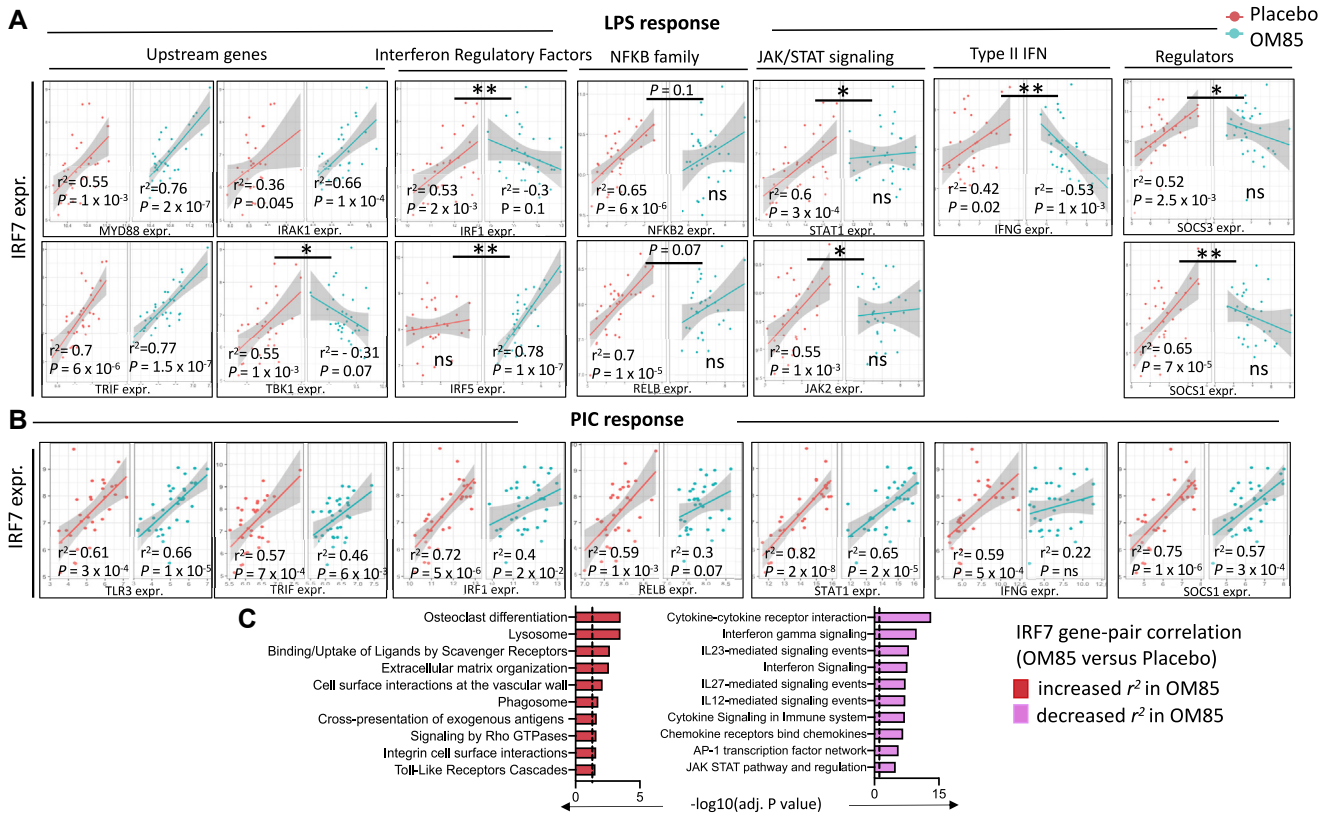

FIG 6. Expression correlation patterns for IRF7 after OM85 treatment (*turquoise*) or placebo (*red*). For each comparison, IRF7 is on the *y-axis,* and known key signaling genes in the innate response are on the *x-axis* for LPS/PIC (**A** and **B**). A linear model was fit to the data in each comparison, with the *gray lines* representing 95% confidence intervals and r^2, Pearson correlation. $P < .05$ was deemed significant for gene-pair correlations within group; *ns,* not significant. Significance of the different correlation patterns between groups was assigned using 100 permutations of the data. Adjusted $*P < .05$, $**P < .005$. **C**, Pathways enriched in genes that had a significant increase (n = 412, *red*) and decrease (n = 329, *pink*) in expression correlation with IRF7 using InnateDB.

IL10 were central module C hubs in both groups. However, in the treatment group, these hubs had a reduced number of connections, and at the protein expression level, top hubs (IL-6, IL-1β, CCL3, IL-10) trended lower in the treatment group (Fig 2). Additionally, there were a number of genes that served as module C hubs in the placebo network that were either completely absent from the corresponding OM85 network (eg, *NFKBIA, VEGFA, CEBPB, CD44*) (see Fig E8 in the Online Repository available at www.jacionline.org).

Differential gene correlation analysis

The WGCNA analyses above characterized global gene network patterns underlying innate immune responses in the placebo and OM85 groups. To elucidate differential network wiring between the respective responses more locally at the level of individual gene pairs, we performed DGCA using the R package DGCA. We focused these analyses on key molecules that orchestrate *TLR4* signaling (eg, *TLR4, MYD88*) and their downstream effectors (transcription factors, proinflammatory cytokines, IFN-stimulated genes). In the posttreatment LPS response network of the OM85 group but not in placebo, *TLR4* correlated positively with downstream adaptors (*MYD88* and *TRIF*), the master IFN pathway regulator *IRF7*, and numerous IFN-stimulated genes (exemplified by *LY6E, ISG15,* and *IFNβ1;* see Fig E9, *A,* in the Online Repository available at www.jacionline.org). Of additional note, *MYD88* correlated inversely with downstream inflammatory cytokine genes (*IL-1, IL-6, IL-18R*; Fig E9, *B*). We ran 100 permutations of the data to compare median changes in correlation between groups, which confirmed that the correlation of *TLR4* with *IRF7* was significantly increased in the OM85 group compared to placebo ($P < .05$). Strikingly, *IRF7* itself was differentially correlated with 741 genes across the OM85 LPS responses (Fig 6, *A,* and see Table E13 in the Online Repository). To demonstrate that the differences in network structure were robust, we repeated the analysis across 10 folds by removing 10% of the data for each fold, and we found that the data were unchanged (see Tables E13 and E14 in the Online Repository). These included multiple inflammatory genes (*CXCR6, IFNγ, IL-6, PTGS2*) and negative regulators of type 1/2/3 IFN and cytokine signaling (*SOCS1, SOCS3*) showing reduced correlation, and a number of additional pathogen/pattern recognition receptors (*CLEC7A, CLEC4A*), which showed increased correlation. Notably, *CLEC7A* was earlier identified as an upstream driver of the LPS response in the OM85 groups (Fig 4, *F*). In contrast, there were no significant differences in *TLR3* or *IRF7* gene-pair correlations in the corresponding PIC responses (Fig 6, *B,* and Table E13). These findings are suggestive

of heightened pathogen sensing capability and reduced inflammatory responses to LPS in the OM85 group. Consistent with this, pathway analysis of the 741 *IRF7*-associated genes revealed reciprocal patterns of change in relevant pathways (Fig 6, *C*).

As mentioned earlier, the coexpression network in the OM85 treatment group contained a module (module B) that appeared to have arisen via relocation of a subset of genes from module A. Using DGCA, we demonstrated that *TNF* and *MYD88* (and a number of key genes in module B) do not correlate with *IFNγ,* the top hub gene in module A, in the OM85 treatment group as they do in placebo (see Fig E7, *B,* and Table E15 in the Online Repository at www.jacionline.org).

Treatment effects on Treg levels

A consistent observation from previous preclinical studies has been upregulation of baseline Treg levels after OM85 treatment,[17,19,20] and flow cytometric screening demonstrated that this was also a component of the OM85 treatment–associated phenotype in our study group (see Fig E10 in the Online Repository available at www.jacionline.org).

DISCUSSION

The core aim of this study was to elucidate IT-associated mechanisms underlying the protective effects of OM85 treatment in infants across the high-infection-risk winter period. We focused on PBMC cytokine and transcriptomic responses to the virus/bacteria mimics PIC/LPS. Cytokine responses indicated that OM85 treatment reduced proinflammatory responses to LPS. Conventional transcriptomic analyses to identify differentially expressed genes or pathways, and URA to identify upstream molecular drivers, indicated treatment-associated effects that mainly influenced LPS responses. To characterize the nature of these changes in more detail, we used comparative WGCNA analyses to characterize the global topology and connectivity structure of the gene networks underlying PIC/LPS responses in treatment and placebo groups. This was followed by DGCA to provide a finer-grained picture that focuses on differential network wiring at the level of individual gene pairs. This revealed that at 24 hours after stimulation, the global architecture of the innate antimicrobial response network differed between the placebo and OM85 treatment groups, as evidenced by disparities in the number and complexity of respective coexpression modules, as well as their expression within LPS and PIC responses (Fig 5, *A* and *D*).

The most highly responsive module across the networks was interferon module A, the expression profiles of which were dominated in both groups by genes associated with type 1/2/3 IFN-related functions (Fig 5, *C*). Upregulation of this module in the PIC response was common to both groups. However, for the LPS response, this was restricted to the OM85 treatment group, consistent with treatment-associated enhancement of their innate antibacterial defenses. A further notable difference was the rewiring of module A in the OM85 treatment group. This involved relocation of the *TNF* component of the so-called interleukin signaling signature, which is evident within the module A expression profiles (Fig 5, *A* and *B*) into a separate module B, together with a number of other genes associated with induction of antiviral defense/IFN signaling and cell trafficking. In biological terms, this suggests that while the production of IFNs (in particular IFN-γ) and *TNF* are highly correlated within the innate immune response network in infants in the placebo group wherein they function as the 2 most highly connected hub genes in the module A subnetwork, these activities are uncoupled in the corresponding treatment group response network (Fig E7).

This has important implications in relation to understanding intergroup differences in innate immune responses to mixed viral/bacterial infections after treatment, given the well-recognized effects of TNF/IFN-γ interactions on antimicrobial immunity. In this regard, IFN-γ–mediated priming of key macrophage effector functions, including phagocytosis, pathogen killing, and cytokine production/secretion, plays a key role in mobilizing host defenses during the early stages of infection.[33-36] TNF-α been shown to synergize with IFN-γ to amplify this priming effect if these cytokines are coproduced in synchrony.[34,36,37] This can accelerate development of peak pathogen killing capacity in macrophages, but it carries the added risk of exaggerating ensuing inflammatory responses,[36,38,39] particularly secretion of proinflammatory cytokines, including TNF itself.[33] The coexpression of these 2 cytokines, as per the placebo group, would thus set the stage for these interactions to occur. In this regard, we have reported elsewhere that exaggerated IFN signaling is a defining feature of inflammatory responses in PBMC and airway tissues of infants manifesting severe lower respiratory symptoms associated with lower respiratory tract infections, and further that IFN-γ and TNF were prominent among the upstream drivers of these response.[6,7]

Synergy between IFN-γ/TNF-α in the context of bacterial infections has also been reported to mediate disruption of airway epithelial barrier function,[40] which is among the recognized sequelae of severe respiratory infections. Similar observations have been reported in relation to gastrointestinal tract inflammation,[41] where the mechanism appears to involve IFN-γ–mediated upregulation of TNF-α R1/R2 on target epithelial cells. Moreover, localization of *TNF* within network module A in placebo subjects could also compromise the type 1 IFN component of their responses, given that TNF can both inhibit the generation of plasmacytoid dendritic cells (the principal source of type 1 IFNs)[42,43] from their $CD34^+$ progenitors,[44] and can also blockade the virus-triggered release of these IFNs from preactivated plasmacytoid dendritic cells.[44] In contrast, in the OM85 treatment group response in which *TNF* is localized within a separate coexpression subnetwork B, the likelihood of these interactions occurring would logically be reduced.

Module B is downregulated in the LPS response network in the treatment group, which may thus result in lowering these patients' risk of proinflammatory sequelae during bacterial clearance while being reciprocally upregulated within the corresponding response to the virus mimic PIC. The coexpressed genes within PIC response module B include many associated with IFN signaling, cell trafficking, and/or TLR function, which are presumably complementary to others mediating similar functions that are activated within the parallel network module A. In principle, this provides a framework to explain how OM85 treatment may achieve a more balanced type 1/2 IFN-dependent response to both types of pathogen in which excessive proinflammatory IFN-γ/TNF priming interactions and TNF-mediated interference with type 1 IFN functions are minimized. However the treatment-mediated network rewiring process, as illustrated in Fig 5, *B,* also involved remodeling of a number of other coexpression

modules. The most important of these is module C, which is upregulated in the LPS response in both groups and encompasses a broad range of genes other than TNF that are recognized as proinflammatory. In this case, rewiring of the treatment group response involved relocation of >50% of the genes present in this subnet in the placebo group to other modules that are downregulated within the network, and more importantly resulted in uncoupling expression of a range of proinflammatory genes (exemplified by *IL-1, IL-6*) from the key nuclear factor kappa–light-chain enhancer of activated B cells pathway (Fig E8) through which they signal to mediate their effects.[45] These inflammatory gene module changes are consistent with the reduced capacity for LPS-induced inflammatory cytokine production in the OM85 group, mirroring findings from animal model studies.[17] It is additionally noteworthy that asthma protection resulting from early-life exposure to microbe-rich traditional farming environments, a process that could be considered a natural form of IT,[12] has also been associated with reduced proinflammatory responses to LPS *in vitro*.[46-48]

In conclusion, this study suggests that the main target for the IT-associated effects of OM85 treatment may be innate immune pathways that primarily regulate host responses to bacterial as opposed to viral pathogens. However, this is unlikely to limit the potential effectiveness of IT for sLRI control, given that the nasopharyngeal microbial milieu during sLRIs almost invariably comprises a mixture of both pathogen classes, which appear to interact synergistically to drive infection spread and symptom severity.[1-3]

This study has several limitations, including sample size, lack of information on the presence and/or identity of bacterial pathogens, and single time point assessment of innate immune responses. Stratification of groups on the basis of infection susceptibility was not possible because of the sample size and requires addressing in future studies. Additionally, the study involved a high-risk cohort and needs to be repeated in an unselected population. Moreover, while there are an expanding number of precedents for suggesting a key role[49] in immune modulation for gene network rewiring in the absence of overt changes in differential expression profiles,[49-51] the contribution of different cell populations in such processes remains obscure. In this regard, animal model studies suggest that myeloid precursor cells may be key targets for OM85-mediated IT effects,[18,19] and this possibility merits follow-up that uses recently developed single-cell RNA sequencing technologies.[52]

We thank the parents and study participants.

Key messages

- **OM85 treatment in infancy induced immune changes indicative of innate IT.**
- **Treatment primarily modulates gene networks triggered during innate immune responses to bacterial pathogens that typically accompany viral pathogens during sLRI.**
- **IT treatment effects include upregulation of IRF7-dependent IFN signaling and increased coordination with innate pathogen-sensing functions, accompanied by attenuation of potentially pathogenic inflammation.**

REFERENCES

1. Teo SM, Mok D, Pham K, Kusel M, Serralha M, Troy N, et al. The infant nasopharyngeal microbiome impacts severity of lower respiratory infection and risk of asthma development. Cell Host Microbe 2015;17:704-15.
2. Teo SM, Tang HHF, Mok D, Judd LM, Watts SC, Pham K, et al. Airway microbiota dynamics uncover a critical window for interplay of pathogenic bacteria and allergy in childhood respiratory disease. Cell Host Microbe 2018;24:341-52.e5.
3. Tang HHF, Lang A, Teo SM, Judd LM, Gangnon R, Evans MD, et al. Developmental patterns in the nasopharyngeal microbiome during infancy are associated with asthma risk. J Allergy Clin Immunol 2021;147:1683-91.
4. Levy O, Ramilo O, Gans H, King C, PrabhuDas M, Adkins B, et al. Challenges in infant immunity: implications for responses to infection and vaccines. Nat Immunol 2011;12:189-94.
5. Holt PG, Mok D, Panda D, Renn L, Fabozzi G, deKlerk NH, et al. Developmental regulation of type 1 and type 3 interferon production and risk for infant infections and asthma development. J Allergy Clin Immunol 2019;143:1176-82.e5.
6. Jones AC, Anderson D, Galbraith S, Fantino E, Cardenas DG, Read JF, et al. Immunoinflammatory responses to febrile lower respiratory infections in infants display uniquely complex/intense transcriptomic profiles. J Allergy Clin Immunol 2019;144:1411-3.
7. Jones AC, Anderson D, Galbraith S, Fantino E, Gutierrez Cardenas D, Read JF, et al. Personalized transcriptomics reveals heterogeneous immunophenotypes in children with viral bronchiolitis. Am J Respir Crit Care Med 2019;199:1537-49.
8. Holt PG, Sly PD. Viral infections and atopy in asthma pathogenesis: new rationales for asthma prevention and treatment. Nat Med 2012;18:726-35.
9. Martinez FD. Early-life origins of chronic obstructive pulmonary disease. N Engl J Med 2016;375:871-8.
10. Levy O, Wynn JL. A prime time for trained immunity: innate immune memory in newborns and infants. Neonatology 2014;105:136-41.
11. Netea MG, Quintin J, Meer JWMvd. Trained immunity: a memory for innate host defense. Cell Host Microbe 2011;9:355-61.
12. Holt PG, Strickland DH, Custovic A. Targeting maternal immune function during pregnancy for asthma prevention in offspring: harnessing the "farm effect"? J Allergy Clin Immunol 2020;146:270-2.
13. Schaad UB. OM-85 BV, an immunostimulant in pediatric recurrent respiratory tract infections: a systematic review. World J Pediatr 2010;6:5-12.
14. Esposito S, Soto-Martinez ME, Feleszko W, Jones MH, Shen KL, Schaad UB. Nonspecific immunomodulators for recurrent respiratory tract infections, wheezing and asthma in children: a systematic review of mechanistic and clinical evidence. Curr Opin Allergy Clin Immunol 2018;18:198-209.
15. Oral bacterial extract for the prevention of wheezing lower respiratory tract illness (ORBEX). ClinicalTrials.gov. https://clinicaltrials.gov/ct2/show/NCT02148796.
16. Sly PD, Galbraith S, Islam Z, Holt B, Troy N, Holt PG. Primary prevention of severe lower respiratory illnesses in at-risk infants using the immunomodulator OM-85. J Allergy Clin Immunol 2019;144:870-2.e11.
17. Scott NM, Lauzon-Joset JF, Jones AC, Mincham KT, Troy NM, Leffler J, et al. Protection against maternal infection–associated fetal growth restriction: proof-of-concept with a microbial-derived immunomodulator. Mucosal Immunol 2017;10:789-801.
18. Mincham KT, Jones AC, Bodinier M, Scott NM, Lauzon-Joset JF, Stumbles PA, et al. Transplacental innate immune training via maternal microbial exposure: role of XBP1-ERN1 axis in dendritic cell precursor programming. Front Immunol 2020;11:601494.
19. Mincham KT, Scott NM, Lauzon-Joset JF, Leffler J, Larcombe AN, Stumbles PA, et al. Transplacental immune modulation with a bacterial-derived agent protects against allergic airway inflammation. J Clin Invest 2018;128:4856-69.
20. Strickland DH, Judd S, Thomas JA, Larcombe AN, Sly PD, Holt PG. Boosting airway T-regulatory cells by gastrointestinal stimulation as a strategy for asthma control. Mucosal Immunol 2011;4:43-52.
21. Troy NM, Hollams EM, Holt PG, Bosco A. Differential gene network analysis for the identification of asthma-associated therapeutic targets in allergen-specific T-helper memory responses. BMC Med Genomics 2016;9:9.
22. Leffler J, Read JF, Jones AC, Mok D, Hollams EM, Laing IA, et al. Progressive increase of FcεRI expression across several PBMC subsets is associated with atopy and atopic asthma within school-aged children. Pediatr Allergy Immunol 2019;30:646-53.
23. Anders S, McCarthy DJ, Chen Y, Okoniewski M, Smyth GK, Huber W, et al. Count-based differential expression analysis of RNA sequencing data using R and Bioconductor. Nature Protoc 2013;8:1765-86.

24. Langfelder P, Horvath S. WGCNA: an R package for weighted correlation network analysis. BMC Bioinformatics 2008;9:559.
25. Jones AC, Troy NM, White E, Hollams EM, Gout AM, Ling KM, et al. Persistent activation of interlinked type 2 airway epithelial gene networks in sputum-derived cells from aeroallergen-sensitized symptomatic asthmatics. Sci Rep 2018;8:1511.
26. Veerati PC, Troy NM, Reid AT, Li NF, Nichol KS, Kaur P, et al. Airway epithelial cell immunity is delayed during rhinovirus infection in asthma and COPD. Front Immunol 2020;11:974.
27. Breuer K, Foroushani AK, Laird MR, Chen C, Sribnaia A, Lo R, et al. InnateDB: systems biology of innate immunity and beyond—recent updates and continuing curation. Nucleic Acids Res 2013;41(Database issue):D1228-33.
28. Yu G, He QY. ReactomePA: an R/Bioconductor package for reactome pathway analysis and visualization. Mol Biosyst 2016;12:477-9.
29. Krämer A, Green J, Pollard JJ, Tugendreich S. Causal analysis approaches in Ingenuity Pathway Analysis. Bioinformatics 2014;30:523-30.
30. McKenzie AT, Katsyv I, Song WM, Wang M, Zhang B. DGCA: a comprehensive R package for differential gene correlation analysis. BMC Syst Biol 2016;10:106.
31. Weichhart T, Costantino G, Poglitsch M, Rosner M, Zeyda M, Stuhlmeier KM, et al. The TSC-mTOR signaling pathway regulates the innate inflammatory response. Immunity 2008;29:565-77.
32. Amit I, Garber M, Chevrier N, Leite AP, Donner Y, Eisenhaure T, et al. Unbiased reconstruction of a mammalian transcriptional network mediating pathogen responses. Science 2009;326(5950):257-63.
33. Hayes MP, Freeman SL, Donnelly RP. IFN-gamma priming of monocytes enhances LPS-induced TNF production by augmenting both transcription and MRNA stability. Cytokine 1995;7:427-35.
34. Ma J, Chen T, Mandelin J, Ceponis A, Miller NE, Hukkanen M, et al. Regulation of macrophage activation. Cell Mol Life Sci 2003;60:2334-46.
35. Salim T, Sershen CL, May EE. Investigating the role of TNF-α and IFN-γ activation on the dynamics of iNOS gene expression in LPS stimulated macrophages. PLoS One 2016;11:e0153289.
36. Schroder K, Hertzog PJ, Ravasi T, Hume DA. Interferon-gamma: an overview of signals, mechanisms and functions. J Leukoc Biol 2004;75:163-89.
37. Parameswaran N, Patial S. Tumor necrosis factor-α signaling in macrophages. Crit Rev Eukaryot Gene Expr 2010;20:87-103.
38. Chousterman BG, Swirski FK, Weber GF. Cytokine storm and sepsis disease pathogenesis. Semin Immunopathol 2017;39:517-28.
39. Mosser DM, Edwards JP. Exploring the full spectrum of macrophage activation. Nat Rev Immunol 2008;8:958-69.
40. Coyne CB, Vanhook MK, Gambling TM, Carson JL, Boucher RC, Johnson LG. Regulation of airway tight junctions by proinflammatory cytokines. Mol Biol Cell 2002;13:3218-34.
41. Wang F, Schwarz BT, Graham WV, Wang Y, Su L, Clayburgh DR, et al. IFN-gamma–induced TNFR2 expression is required for TNF-dependent intestinal epithelial barrier dysfunction. Gastroenterology 2006;131:1153-63.
42. Siegal FP, Kadowaki N, Shodell M, Fitzgerald-Bocarsly PA, Shah K, Ho S, et al. The nature of the principal type 1 interferon-producing cells in human blood. Science 1999;284(5421):1835-7.
43. Cella M, Jarrossay D, Facchetti F, Alebardi O, Nakajima H, Lanzavecchia A, et al. Plasmacytoid monocytes migrate to inflamed lymph nodes and produce large amounts of type I interferon. Nat Med 1999;5:919-23.
44. Palucka AK, Blanck JP, Bennett L, Pascual V, Banchereau J. Cross-regulation of TNF and IFN-alpha in autoimmune diseases. Proc Natl Acad Sci U S A 2005; 102:3372-7.
45. Liu T, Zhang L, Joo D, Sun SC. NF-κB signaling in inflammation. Signal Transduct Target Ther 2017;2:17023.
46. Kirjavainen PV, Karvonen AM, Adams RI, Täubel M, Roponen M, Tuoresmäki P, et al. Farm-like indoor microbiota in non-farm homes protects children from asthma development. Nat Med 2019;25:1089-95.
47. Stein MM, Hrusch CL, Gozdz J, Igartua C, Pivniouk V, Murray SE, et al. Innate immunity and asthma risk in Amish and Hutterite farm children. N Engl J Med 2016;375:411-21.
48. Ege MJ, Mayer M, Normand AC, Genuneit J, Cookson WOCM, Braun-Fahrländer C, et al. Exposure to environmental microorganisms and childhood asthma. N Engl J Med 2011;364:701-9.
49. Jones AC, Anderson D, Troy NM, Mallon D, Hartmann R, Serralha M, et al. Rewiring of gene networks underlying mite allergen-induced $CD4^+$ Th-cell responses during immunotherapy. Allergy 2020;75:2330-41.
50. de la Fuente A. From "differential expression" to "differential networking"—identification of dysfunctional regulatory networks in diseases. Trends Genet 2010;26:326-33.
51. Hudson NJ, Dalrymple BP, Reverter A. Beyond differential expression: the quest for causal mutations and effector molecules. BMC Genomics 2012;13:356.
52. Chen G, Ning B, Shi T. Single-cell RNA-Seq technologies and related computational data analysis. Front Genet 2019;10:317.